

COHERENT HARMONIC GENERATION AT THE DELTA STORAGE RING*

H. Huck[†], M. Bakr, M. Höner, S. Khan, R. Molo, A. Nowaczyk,
A. Schick, P. Ungelenk, M. Zeinalzadeh,

Zentrum für Synchrotronstrahlung, TU Dortmund University, 44221 Dortmund, Germany

Abstract

First commissioning results from a new Coherent Harmonic Generation (CHG) source, recently installed at the DELTA storage ring, are presented. DELTA, a university-operated synchrotron light source in Dortmund, has successfully operated an optical klystron as storage-ring FEL [1]. After installing a Ti:sapphire laser system and new undulator power supplies earlier this year, the optical klystron can be seeded using ultrashort pulses at 800 nm wavelength during standard operation of the storage ring at 1.5 GeV. The energy modulation induced within a short slice of an electron bunch is converted into a density modulation and the micro-bunched electrons emit ultrashort pulses coherently at harmonics of the initial wavelength. Several meters downstream of the optical klystron, path length differences of the energy-modulated electrons cause a dip in the charge distribution, giving rise to coherent ultrashort THz pulses which are extracted using a dedicated beamline.

INTRODUCTION

Several methods to create sub-picosecond pulses of VUV and X-ray radiation provide means to study ultra-fast phenomena on the atomic scale, e.g. phase transitions, chemical reactions or demagnetization of magnetic materials. At several storage rings [2, 3, 4], a femtosecond laser pulse co-propagating with an electron bunch in an undulator (“modulator”) is used to imprint an energy modulation onto a short slice of the bunch. After parts of this slice have been transversely displaced by dispersive elements, ultrashort X-ray pulses are generated in a subsequent undulator [5]. However, such “slicing” sources produce a low photon rate since only a small fraction of electrons in the bunch contribute. In the Coherent Harmonic Generation (CHG) scheme (Fig. 1), an energy-modulated electron slice is created in the same way. In contrast to slicing sources, a subsequent dispersive chicane transforms the energy modulation into a density modulation. The resulting microbunches radiate coherently in a second undulator (“radiator”). Since the electron distribution of the modulated slice has a rich harmonic content, the radiator can be tuned to provide ultrashort pulses typically up to the 5th harmonic. Even shorter wavelengths are achievable

by e.g. frequency-up conversion of the external laser, or by Echo-Enabled Harmonic Generation (EEHG) [11].

CHG at storage rings was demonstrated first at ACO [6], and more recently at Elettra [7] and UVSOR II [8]. At DELTA, a new CHG source has now been successfully commissioned in standard routine operation.

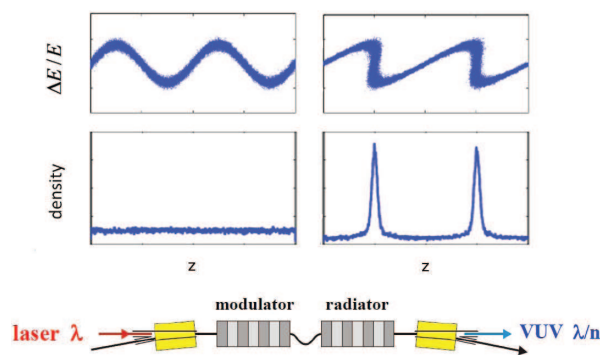


Figure 1: Principle of Coherent Harmonic Generation. An energy modulation is imprinted onto the electron bunch by a co-propagating laser pulse in the modulator. After conversion into a density modulation by a dispersive chicane, the micro-bunched electrons radiate coherently in the radiator at harmonics of the laser wavelength.

DELTA is a synchrotron light source with a nominal beam energy of 1.5 GeV and a circumference of 115.2 m (Fig. 2). The electromagnetic undulator U250 in the northern straight section consists of 19 periods of 25 cm each, and was in the past used as optical klystron for storage-ring FEL studies. New power supplies allow separate tuning of the first and last part to undulator parameters up to $K=12$, whereas the three central periods serve as a dispersive chicane with magnetic fields up to 0.76 T.

SETUP

Pulses from a Ti:sapphire laser system (max. 8 mJ at 1 kHz, 35 fs) are sent and focused via beamline BL3 into the U250 undulator (Fig. 2). The position and size of the laser waist can be changed by two remote-controlled mirrors and an adjustable telescope. Five meters downstream from the undulator, a water-cooled copper mirror can be moved into the undulator radiation beam to guide it into a diagnostics hutch (BL4). The hutch comprises a streak camera and photodiodes for longitudinal diagnos-

* Work supported by DFG (INST 212/236-1 FUGG), BMBF (05K10PE1, 05K10PEB), and the Federal State NRW

[†] holger.huck@tu-dortmund.de

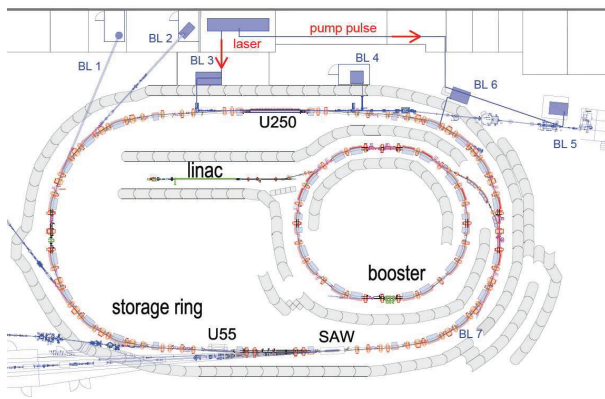


Figure 2: Overview of the DELTA accelerator complex.

tics, a spectrometer, and two CCD cameras with different focal lengths to control the transverse overlap of the laser and electron beam.

Beamline BL5, operated by the Forschungszentrum Jülich, uses VUV pulses from the U250 for spin- and angle-resolved photoelectron spectroscopy. In order to enable pump-probe experiments, a pump-pulse beamline is under construction that will send a fraction of each laser pulse with a variable delay relative to the CHG pulse to the experimental station.

Approximately 13 m downstream from the undulator, dispersive effects have displaced the off-energy electrons in the modulated slice of the bunch far enough to leave a gap (approx. 100 μm) in the bunch profile, giving rise to coherent THz radiation. This THz radiation is extracted through a dedicated beamline (BL6) and detected by a liquid He-cooled hot-electron bolometer.

COMMISSIONING

During the first week of machine operation dedicated to this project, the first coherent THz and CHG pulses were observed in single-bunch mode. A few shifts later, an electron orbit was established that complies with both standard user and CHG operation, and CHG was successfully demonstrated during user shifts with a multi-bunch filling pattern and a few bunches with increased charge. The commissioning parameters are listed in Tab. 1.

Table 1: CHG Commissioning Parameters

laser wavelength	795 nm
pulse duration	50 fs (FWHM)
repetition rate	1 kHz
used pulse energy	2 mJ
laser waist	0.27 mm (rms)
radiator wavelength	400 nm
electron energy	1.5 GeV
bunch length	95 ps (FWHM)
bunch charge (current)	< 4 nC (10 mA)

Alignment

To create the required overlap of laser pulses and electron bunches, the following routine is used. After setting the telescope to the desired laser waist diameter, the laser beam is centered on two screens in BL3 and on the exit window of BL4. The transmitted laser power in the diagnostics hutch is optimized by further transverse adjustments. The laser light and synchrotron radiation are then focused onto a fast photodiode to coarsely adjust the timing for one particular bunch before fine-tuning it using a streak camera and an RF phase shifter. Finally, two CCD cameras with different focal lengths are used to observe and adjust the transverse overlap of the laser pulses and electrons. Once a THz signal is observed, indicating a reasonable energy modulation, this signal serves as reliable indicator to further improve and maintain the longitudinal and transverse overlap.

By scanning the electron bunch with the laser, the THz signal can also be used to measure the bunch dimensions indirectly. An example is shown in Fig. 3 for the longitudinal case. The measured width of 67 ps (FWHM) corresponds to a bunch length of 95 ps, since the signal is proportional to the squared electron density. This value is slightly larger than the natural bunch length of 85 ps, as it should be due to turbulent bunch lengthening at a bunch current of 3.7 mA.

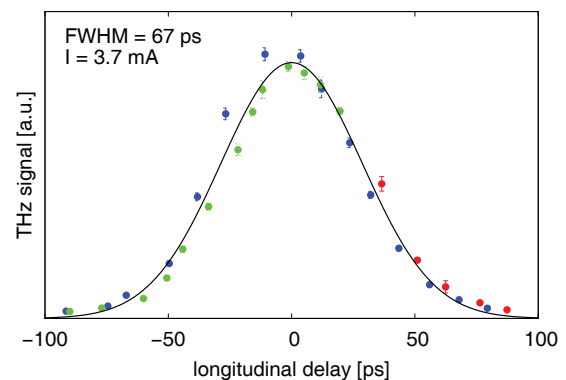


Figure 3: THz radiation vs. longitudinal delay. The small error bars on the slopes indicate a small short-term jitter, but there is a slight long-term drift between the three scans (red/green/blue dots) done within one hour.

Coherent Radiation

The intensity of coherent synchrotron radiation is proportional to the square of the number of electrons. Accordingly, the measured coherent THz signal grows quadratically with the bunch current (Fig. 4) for wavelengths comparable or longer than the gap in the electron distribution.

The CHG signal and spontaneous undulator radiation around 400 nm was measured using a photodiode and an oscilloscope after blocking the intense laser pulses by a dielectric mirror (transmission at 800 nm below 0.1%) and a

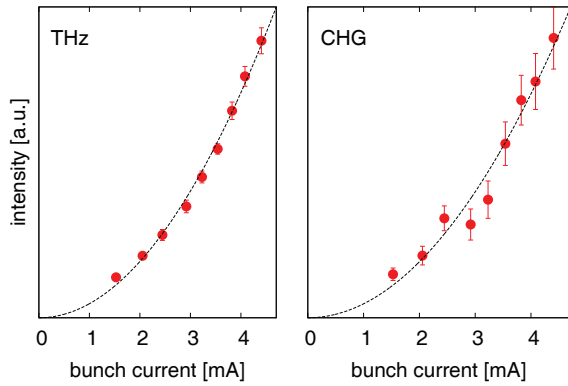


Figure 4: The measured intensity of the coherent THz radiation (left) and the CHG radiation (right) is proportional to the square of the bunch current.

bandpass filter ($400 \text{ nm} \pm 25 \text{ nm}$). Both the CHG signal and spontaneous radiation of the next roundtrip in the storage ring were measured. The coherent nature of the CHG signal was confirmed by the quadratic dependence on the beam current (Fig. 4).

CHG Spectrum

The radiation spectrum around 400 nm was measured with a Czerny-Turner-type spectrometer and a photomultiplier at its exit slit. The spectrum of the spontaneous emission (Fig. 5) can be explained qualitatively. The shape stems from the interference of radiation from the three differently tuned undulator parts (modulator, chicane, radiator) with matching sections and a finite angular and energy distribution.

The CHG pulse itself (Fig. 5 bottom curve) has a FWHM width of only 5 nm, indicating a time-bandwidth product close to the Fourier limit.

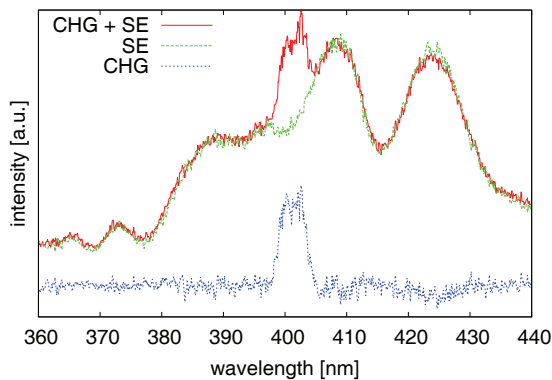


Figure 5: Measured undulator spectrum with and without CHG signal (top curves). The difference (bottom curve) is the pure CHG spectrum.

BUNCHING FACTOR

It is imperative that the maximum energy modulation stays below the energy acceptance of the storage ring, which in the case of DELTA is limited by the accelerating RF to $\Delta E/E \approx 0.9\%$. Simulations show that this value can be reached with 2 mJ of laser power inside the modulator, provided perfect alignment of overlap and a laser waist size of 0.4 mm (rms). The highest CHG power $P(\lambda)$ at a given wavelength λ is not necessarily achieved with the maximum energy modulation, but rather with the maximum bunching factor $b(\lambda)$, which is the Fourier transform of the electron density. The total radiation power of N electrons compared to that of a single electron P_1 can be written as [10]

$$P(\lambda) = P_1(\lambda) [N + N_b^2 b^2(\lambda)], \quad (1)$$

where N_b is the number of electrons in the slice over which the bunching factor is averaged, in our case $(N_b/N) \approx (40 \text{ fs}/100 \text{ ps})$ for a single bunch.

Simulations using a modified version of the code *elegant* [9] that take the transverse dimensions and wiggling of the electron bunch as well as a beam quality factor $M^2 = 2$ for the laser into account, confirm an optimum laser waist of $\sigma = 0.4 \text{ mm}$ (Fig. 6). During commissioning, the real laser waist was astigmatic and significantly smaller ($\sigma = 0.27 \text{ mm}$) in the horizontal plane, thus reducing the Rayleigh length and the bunching factor by approx. 15%. Once the waist in both planes is fixed to the optimum value and M^2 approaches the nominal value (< 1.5), we expect an increase in the bunching factor of approx. 30%.

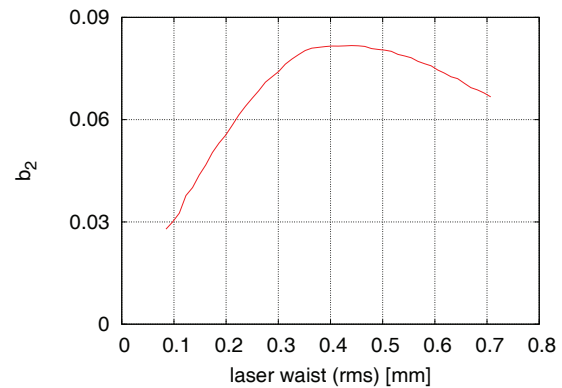


Figure 6: Bunching factor of the second harmonic versus laser waist size inside the modulator (pulse energy 1.7 mJ, $M^2=2$).

According to Eq. 1, the achieved bunching factor can be estimated from the ratio between the measured coherent and incoherent radiation. The measurement of CHG power versus chicane strength (Fig. 7) was taken at a bunch current of approx. 4 mA ($N=9.5 \cdot 10^9$). At maximum strength the CHG signal was six times higher than the spontaneous radiation, which translates into a bunching factor of $b_2^2 = (6 \cdot (N/N_b)^2/N)$ or $b_2 = 0.063$ at 400 nm.

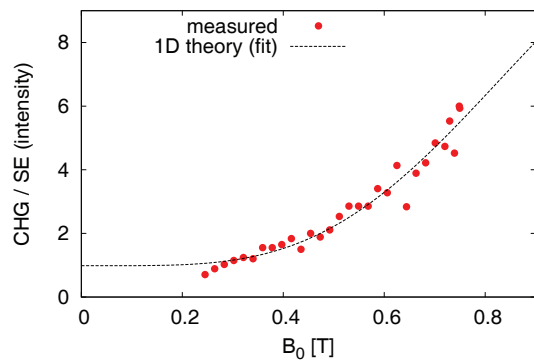


Figure 7: Measured ratio of CHG to spontaneous radiation intensity versus chicane coil current.

This value is significantly lower than what can be expected using a stronger chicane, as simulations show in Fig. 8. At the nominal beam energy of 1.5 GeV and a modulation wavelength of 800 nm, optimum microbunching would require a maximum magnetic field of 1.4 T in the current antisymmetric chicane, whereas the coils are thermally limited to 0.76 T. This can be solved by changing the polarity of some coils, thus creating a symmetric chicane, which achieves more than twice the present R_{56} with the maximum coil current. However, it is intended to reduce the CHG wavelength by seeding the modulator with frequency-tripled laser pulses. In this case, a modification of the chicane is not necessary, since the R_{56} required for optimum microbunching decreases linearly with the wavelength.

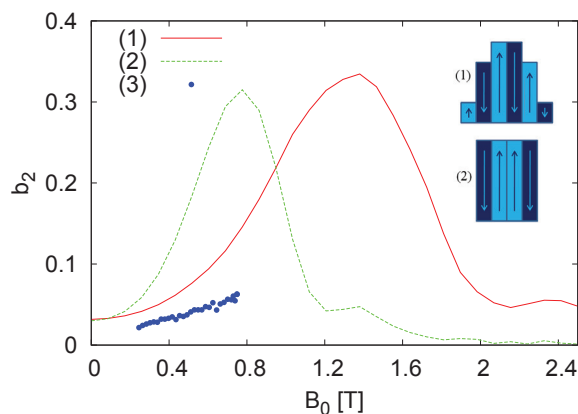


Figure 8: Bunching factor of the second harmonic versus peak magnetic field, comparing the current antisymmetric chicane configuration (1) with a symmetric one (2). The blue dots (3) correspond to the data depicted in Fig. 7.

OUTLOOK

The goal of the project is to provide ultrashort VUV pulses at wavelengths below 100 nm in standard user operation. Since the bunching factor decreases exponentially

with the harmonic number, the next step is to seed the modulator with 266 nm pulses, using a third-harmonic conversion (THG) unit after the Ti:sapphire amplifier. This will both alleviate the effect of electron wiggling inside the laser field and reduce the required R_{56} value for optimum microbunching. Users at BL5 can expect a reasonable photon flux up to the 5th harmonic (53 nm). Optionally, the central wavelength will be adjustable via simultaneous tuning of an optical parametric amplifier (OPA) and the undulator coil currents.

An increase of CHG-pulse intensity during standard user operation is expected due to the commissioning of a new electron gun at the DELTA storage ring this summer. This will enable a reliable hybrid filling pattern, i.e. a distinct single bunch of approx. 10 mA within the gap of a standard three-quarter filling of the storage ring. In addition, a recently installed bunch-by-bunch feedback system will stabilize the electron beam in all three dimensions and consequently increase the average CHG power as well.

To further increase the available photon energy and flexibility of ultrashort pulses at DELTA, several options are being investigated. Downstream from the U250, a slicing undulator and a new dedicated beamline could be installed. Even more appealing might be echo-enabled harmonic generation [11], which has been successfully demonstrated at linacs, e.g. [12], but in principle is applicable for storage rings as well. At DELTA, both slicing and EEHG would require an additional undulator as well as some changes to the vacuum chamber and the lattice [13].

REFERENCES

- [1] D. Nölle et al., Nucl. Inst. Methods A 445, 128 (2000).
- [2] R.W. Schoenlein., Science 287, 2237 (2000).
- [3] S. Khan et al., Phys. Rev. Lett. 97, 074801 (2006).
- [4] P. Beaud et al., Phys. Rev. Lett. 99, 174801 (2007).
- [5] A. Zholents and M. Zolotarev, Phys. Rev. Lett. 76, 912 (1996).
- [6] B. Girard et al., Phys. Rev. Lett. 53, 2405 (1984).
- [7] E. Allaria et al., Phys. Rev. Lett. 100, 174801 (2008).
- [8] M. Labat et al., Phys. Rev. Lett. 101, 164803 (2008).
- [9] M. Borland, Advanced Photon Source LS-287 (2000).
- [10] J. Wu and L. H. Yu, SLAC-PUB-10494 (2004).
- [11] G. Stupakov, Phys. Rev. Lett. 102, 074801 (2009).
- [12] D. Xiang et al., Phys. Rev. Lett. 105, 114801 (2010).
- [13] R. Molo et al., this conference, TUPA19.